Supporting Information

Cellular uptake mechanisms of diselenide-based ROS-responsive nanocarrier in oxidatively stressed colon cells

Table of Contents

Material and methods

Sodium selenocysteine dihydrochloride, N-α-formyl-N-epsilon-tert-butoxycarbonyl-D-lysine, 1-ethyl-3-(dimethylaminopropyl)carbodiimide hydrochloride (EDCI), N-hydroxysuccinimide (NHS), carboxymethyl cellulose (CMC), trifluoroacetic acid, and folic acid were all purchased from Shanghai Macklin Biochemical Technology Co., Ltd. Inhibitors such as Ethylisopropylamiloride (EIPA), Chlorpromazine, Genistein, and Dynasore were purchased from MedChemexpress, a biotechnology company in the United States.

Synthesis of Se-NH_2. The ROS-responsive element was prepared as follows: Details of the synthesis were sourced from Scheme S1 (ESI†). Initially, 2,2'-Diselanediyldiethanamine dihydrochloride (5 g, 0.016 mmol) was dissolved in 100 mL DMF at 0°C, and stirred for 10 min. After complete dissolution, 5.7 mL N-methyl morpholine was added and stirred for 5 min. Subsequently, N-α-Phthalimido methyl-N-epsilon-t-butyloxycarbonyl-D-lysine (17.82 g, 0.038 mmol) was added to the solution and stirred for 10 min. Lastly, 1-hydroxyphenylpropanetriazole (2.332 g, 0.0173 mmol) and EDC (9.933 g, 0.052 mmol) were added. After 20 min of stirring, the reaction was left to proceed overnight at room temperature.

After the reaction, the mixture was transferred to a separatory funnel and extracted with a mixture of ethyl acetate and water. The upper organic phase was collected, and the aqueous phase was re-extracted with ethyl acetate three times. After combining all organic phases, they were evaporated in a rotary evaporator (100 rpm, 40°C) to remove the solvent. The residue was washed with saturated sodium chloride solution twice to eliminate impurities, then anhydrous sodium sulfate was added to remove residual water. Further purification was achieved by recrystallization. Methanol was added to dissolve the product, followed by dichloromethane to become turbid. The mixture was left at room temperature for 24 h to allow crystal formation. The light-yellow solid, identified as Se-NHBoc, was filtered and dried.

Se-NHBoc was dissolved in dichloromethane and reacted with a fourfold excess of trifluoroacetic acid for 6 h. Subsequently, sodium bicarbonate was added to neutralize residual trifluoroacetic acid, ceasing when effervescence stopped. The product, Se-NH_2, was filtered, dried, and stored at 4°C for future use. The structure was confirmed by ^{1}H-NMR spectroscopy using a Varian 500 MHz instrument.

Synthesis of CMC-Se, Cy5.5-CMC-Se and Cy5.5-CMC. Using sodium selenocysteine dihydrochloride as the starting material, it reacts with N-α-formyl-N-epsilon-tert-butoxycarbonyl-D-lysine to yield the intermediate product Se-NHBoc. Next, trifluoroacetic acid is used to remove the Boc protecting group, resulting in the final product Se-NH_2. Subsequently, under the catalysis of NHS and EDCI, the synthesized Se-NH_2 is used to modify the carboxyl groups on the side chains of carboxymethyl cellulose (CMC). Finally, after dialysis and freeze-drying treatment, a light yellow fibrous solid, CMC-Se, is obtained (see reaction pathway in Scheme S1).

Under the catalysis of NHS and EDCI, Cy5-NH_2 is conjugated with CMC-Se. After the reaction is completed, the final solid form of Cy5.5-CMC-Se is obtained through dialysis and freeze-drying treatment. Cy5.5-CMC was synthesized in the same way.

ATR-FTIR analysis. The chemical structures of CMC-Se and CMC-Se (with or without 10 mM H_2O_2 for 36 h), were analyzed using ATR-FTIR spectroscopy (Nicolet iS50, Thermo Fisher Scientific, Waltham, MA, USA). The samples were analyzed using transmittance with a spectral range of 4000 to 550 cm^{-1}, 32 scans, and a resolution of 4 cm^{-1}.

X-ray photoelectron spectrometer (XPS) analysis. The binding energy of Se-bonds was investigated using X-ray photoelectron spectroscopy (XPS, K-Alpha, Thermo Fisher Scientific, USA). CMC-Se (with and without 10 mM H_2O_2 for 36 h) were cut to 5×5 mm and mounted on the sample tray and placed into the instrument's sample chamber. Once the sample chamber pressure was below 2.0×10^{-7} mbar, the samples were transferred to the analysis chamber at 400 μm spot size, 12 kV working voltage, and 6 mA filament current; full-spectrum scan energy was 150 eV with a 1 eV step size; narrow-spectrum scan energy was 50 eV with a 0.1 eV step size.

Selenium content and distribution of CMC-Se. The distribution and mass fraction of selenium were characterized using Energy Dispersive X-ray Spectroscopy (EDX) on a Transmission Electron Microscope (TEM; JEOL-200, JEOL Ltd., Tokyo, Japan)

Observation of morphology. The Morphology of CMC-Se (with or without 10 mM H_2O_2 for 36 h) was examined by TEM and Scanning Electron Microscope (SEM; Gemini 300, Carl Zeiss AG, Jena, Germany).

***In vitro* drug release.** Place 50 mL of the sample (CMC-Se or CMC) in a PBS buffer solution (pH 6.8) and introduce varying concentrations of H_2O_2 to achieve final concentrations of 0, 0.5, 1, and 10 mM in the solution. Transfer the samples to a shaking incubator set at 37°C with a shaking speed of 100 rpm. At each designated time point, withdraw 2 mL of the sample, centrifuge at 3000 rpm for 5 min, and collect the supernatant for quercetin content analysis. Replace the removed volume with 2 mL of the corresponding PBS solution. Following absorbance measurement at 374 nm with a UV-Vis spectrophotometer, calculate the release rate using Eqs 1.

Place 50 mL of CMC-Se in a PBS buffer solution a PBS buffer solution (pH 6.8) and introduce varying concentrations of GSH to achieve final concentrations of 0, 1 and 10 mM in the solution. Transfer the samples to a shaking incubator set at 37°C with a shaking speed of 100 rpm. At each designated time point, withdraw 2 mL of the sample, centrifuge at 3000 rpm for 5 min, and collect the supernatant for Curcumin content analysis. Replace the removed volume with 2 mL of the corresponding PBS solution. Following absorbance measurement at 430 nm with a UV-Vis spectrophotometer, calculate the release rate using Eqs 2.

Release rate (%) = The concentration of quercetin in the supernatant/the concentration of quercetin in the original sample × 100 (1)

Release rate (%) = The concentration of curcumin in the supernatant/the concentration of curcumin in the original sample × 100 (2)

Cell line. HT-29 cells and Caco-2 cells were acquired from the National Collection of Authenticated Cell Cultures, supplemented with 10% fetal bovine serum (Tianhang, Zhejiang, China). HT-29 cells were cultured in McCoy's 5A modified medium (Vivacell, Shanghai, China) containing 10% FBS and 1% antibiotics (100 U/mL penicillin and 0.1 mg/mL streptomycin). Caco-2 cells were cultured in DMEM/High Glucose (biochannel, Nanjing, China) containing 10% FBS and 1% antibiotics. Cells were incubated in a CO_2 incubator at 37°C with 5% CO_2 and passaged using trypsin/ethylenediaminetetraacetic acid containing 0.25% EDTA (Beyotime, Shanghai, China).

Establishment of an oxidative stress cell model. The CCK-8 assay kit (NCM, Suzhou, China) and the Reactive oxygen species (ROS) test kit (Yeasen, Shanghai, China) were employed to determine whether the oxidative stress cell model was successfully established. First, the optimal concentration of H_2O_2 for establishing the oxidative stress model was screened using the CCK-8 method. Cells (1×10^4 per well) were evenly seeded in a 96-well plate and incubated overnight in a CO_2 incubator at 37°C with 5% CO_2. Subsequently, cells were treated with different

concentrations of H_2O_2 for 4 h. After discarding the culture medium, a serum-free medium containing 10% CCK-8 was added, and the cells were incubated for 1 h before measuring OD_{450} using a Multifunctional microplate detector (Biotek SynergyH1MF, USA). Then, the cells treated with H_2O_2 were processed according to the DCFH-DA detection protocol, and intracellular ROS levels were assessed using a Multifunctional microplate detector and Inverted fluorescence microscope (Axio Observer 3, ZEISS, Germany).

Cell viability assay. We observed the cytotoxicity of CMC-Se on cells by assessing cell viability. After seeding the cells in a 96-well plate and incubating overnight, different concentrations of CMC-Se were added for co-culturing with cells for 24 h. Cell viability was then measured using the CCK-8 assay.

Reactive oxygen species (ROS) and matrix metalloproteinases (MMP). The ability of CMC-Se to scavenge ROS was investigated using the DCFH-DA assay. HT-29 cells and Caco-2 cells were cultured in a 6-well plate and incubated overnight. After treatment with 400 μM H_2O_2 for 4 h, HT-29 cells were treated with CMC-Se (0, 20, and 50 μg/mL) or CMC (20, and 50 μg/mL) for 2 h. Similarly, After treatment with 800 μM H_2O_2 for 4 h, Caco-2 cells were treated with 300 μg/mL CMC-Se or CMC for 2 h. The cells were washed with PBS and incubated with 10 μM DCFH-DA in the dark for 30 minutes. After washing, the cells were digested and centrifuged, and intracellular fluorescence was detected using BD Accuri C6 Plus flow cytometry (FCM). Alternatively, HT-29 cells on confocal dishes were observed using Laser confocal microscopy microscopy (LSM800, ZEISS, Germany) after the aforementioned treatments.

The reparative effect of CMC-Se on oxidative stress was studied by detecting the mitochondrial membrane potential using the Mitochondrial Membrane Potential Test Kit (Solarbio, Beijing, China). Oxidative stress HT-29 cells treated with H_2O_2 (400 μM, 4 h) were subsequently treated with 0, 20, and 50 μg/mL CMC-Se for 2 h. JC-10 staining solution was then added, and the cells were incubated at 37°C in a 5% CO_2 incubator for 20 minutes. After washing with PBS, the cells were observed under the LSM800 (ZEISS, Germany), or collected for detection using FCM.

Intracellular antioxidant enzyme activity. A total of 2 x 10^5 cells were seeded in each well of a 6-well plate and incubated overnight. After treatment with H_2O_2 (400 μM for 4 h), the cells were washed with PBS. The cells were then co-cultured with different concentrations of CMC-Se (20 and 50 μg/mL) for 2 h. Subsequently, the cells were washed twice with pre-chilled PBS and collected using a cell scraper. After centrifugation to remove the supernatant, a homogenate was added for mixing, followed by another centrifugation to obtain the supernatant. Finally, the protein concentration was measured using the BCA Protein Assay Kit (NCM, Suzhou, China), and the activities of SOD, CAT, and GSH-Px were determined according to the Total Superoxide Dismutase Assay Kit with WST-8 (Beyotime, Shanghai, China), Catalase (CAT) activity detection kit (Solarbio, Beijing, China), Cellular Glutathione Peroxidase Assay Kit with NADPH (Beyotime, Shanghai, China) instructions.

Intracellular uptake of CMC-Se or CMC. CMC-Se or CMC, conjugated with the fluorescent group (Cy5.5-NH_2), was used to evaluate the cellular uptake of CMC-Se or CMC in different states of HT-29 or Caco-2 cells by observing with laser scanning confocal microscopy and flow cytometry. Specifically, normal and oxidatively stressed cells were co-cultured with CMC-Se or CMC for varying time periods. Fluorescent images were then captured using an LSM800 (ZEISS, Germany), or the mean fluorescence intensity was quantified using FCM.

Subsequently, the localization of Cy5.5-CMC-Se at the cell membrane was observed using a laser

scanning confocal microscope, with oxidatively stressed HT-29 cells co-cultured with Cy5.5-CMC-Se (50 μg/mL) for 6 h. Dio was then added to the confocal dish and incubated at 37°C for 1 h. After removing the culture medium and washing with PBS, the cells were stained with Hoechst 33342 (Beyotime, Shanghai, China) to label the nuclei, followed by observation and imaging using the LSM800.

Lysosomal/mitochondrial co-localization. After treating the oxidatively stressed HT-29 cells with H_2O_2 (400 μM, 4 h), the cells were co-cultured with Cy5.5-CMC-Se (50 μg/mL) for 6 h. Lyso-Tracker (Thermo Fisher Scientific, USA) and Mito-Tracker (Yeasen, Shanghai, China) were then added to the confocal dish in different ratios, followed by incubation at 37°C for an additional hour. Following the removal of the culture medium, the cells were washed twice with PBS, treated with Hoechst 33342 (Beyotime, Shanghai, China), and then imaged using the LSM800. Co-localization analysis was conducted using ImageJ.

The effects of inhibitors on cellular uptake. After seeding HT-29 cells in a 6-well plate, the cells were incubated overnight. After treating HT-29 cells with H_2O_2 (400 μM) for 4 h, they were subsequently treated with different concentrations of inhibitors (EIPA, Chlorpromazine, Genistein) for 3 h. Next, the cells were co-cultured with Cy5.5-CMC-Se (50 μg/mL) for 6 h. After incubation, the cells were washed three times with PBS, then digested and collected, and finally analyzed by FCM.

Proteomics. The proteolytic peptides in the samples were analyzed by Orbitrap Lumos mass spectrometer (Thermo Fisher Scientific, MA, USA). This process obtains accurate and iteratively repeatable full mass spectrometry data of a large number of proteins in DIA mode. At the same time, the spectral library constructed by the traditional data dependent acquisition (DDA) model, combined with the use of Spectronaut X (Biognosys AG) software and Uniprot database, realized the qualitative and quantitative analysis of peptides and proteins identified by mass spectrometry. The results of these analyses yield a large number of reliable quantitative data points.

Proteins identified with at least 2 unique peptides and detected in two biological replicates of at least one group were included. Compared with the control group, the identified proteins with p value ≤ 0.05 and fold change ≥ 1.2 were considered as differentially expressed proteins (DEP) by the hypergeometric test. The differential proteins were enriched into the GO database, and the differential membrane proteins were selected. Then the differential membrane proteins were enriched into the KEGG database to find pathways related to Transport and catabolism. The differential proteins on the transport and catabolism pathways were represented by heat maps.

Western Blot. The Western blot test was employed to investigate the effects of H_2O_2 on key protein expression. Membrane proteins were extracted from HT-29 cells using a cell membrane protein extraction kit (Solarbio, Beijing, China) and quantified with a BCA detection kit (NCM, Suzhou, China). Following treatment, the cells were collected, and membrane proteins were extracted using a buffer containing protease and phosphatase inhibitors. The extracts were then separated by electrophoresis on 10% SDS-PAGE gels. After electrophoresis, the protein bands were transferred to a PVDF membrane, which underwent the following procedures: blocking in a 5% BSA solution for 1 hour, incubation with specific primary antibodies overnight at 4°C, and incubation with HRP-conjugated secondary antibodies for 30 min at room temperature. Visualization was achieved using an ECL substrate and a 9000F Mark II camera (Canon, China). Na, K-ATPase was used as an internal control for normalization. Quantitative analysis was performed using AlphaEaseFC software.

The effects of folic acid on cellular uptake. In order to further verify the inhibitory effect of folic acid on the uptake of HT-29 cells, we first established an oxidative stress cell model using H_2O_2 (400 μM, 4 h), followed by a 3-hour treatment with folic acid. After washing with PBS, the cells were co-cultured with Cy5.5-CMC-Se (50 μg/mL) for 6 h, followed by capturing fluorescence images using a laser scanning confocal microscope and quantifying the cell uptake using FCM.

FOLR1 knockdown by small interfering RNA (siRNA). To silence FOLR1 gene expression, FOLR1-specific siRNA (SiFOLR1) and control siRNA (SiNC) were obtained from Sangon Biotech (Shanghai)Co., Ltd. HT-29 cells were transfected with siRNA (SiFOLR1 or SiNC) and Lipofectamine RNAiMAX transfection reagent. The culture medium was changed to OptiMEM 6 hours post-transfection. After 24 h, the cells were treated with H_2O_2 and nanoparticles, followed by imaging using the LSM800. The sequence of SiFOLR1 is 5'- CCUACAAGGUCAGCAACUA -3' and 5'-UAGUUGCUGACCUUGUAGG -3'.

Molecular docking. Molecular docking is a commonly used method to study the interactions between receptors and ligands, aimed at investigating intermolecular interactions and predicting their binding modes and affinities. Molecular docking technology further elucidates the interactions between CMC-Se and FOLR1. The 3D structure of FOLR1 was obtained from the Protein Data Bank (PDB) (http://www.rcsb.org/), and after performing dehydration and hydrogenation operations using the protein visualization software PyMOL, it was saved. The active site Se-NH_2 of CMC-Se was modeled using GaussView and optimized using the semi-empirical computational software MOPAC. The molecular structure of folic acid was downloaded from the PubChem database (https://pubchem.ncbi.nlm.nih.gov/). Docking was performed separately between Se-NH_2, folic acid, and FOLR1 using the AutoDock-Vina software. The docking results were saved, and the receptor-ligand complexes were visualized and analyzed using VMD and LigPlot.

Statistical analysis. All graphs were generated using GraphPad Prism software, and the results are expressed as means. An unpaired Student's t-test was employed for comparisons between the two samples. One-way analysis of variance (ANOVA) and Tukey's post-hoc tests were employed to compare multiple samples. $P < 0.05$ was considered statistically significant.

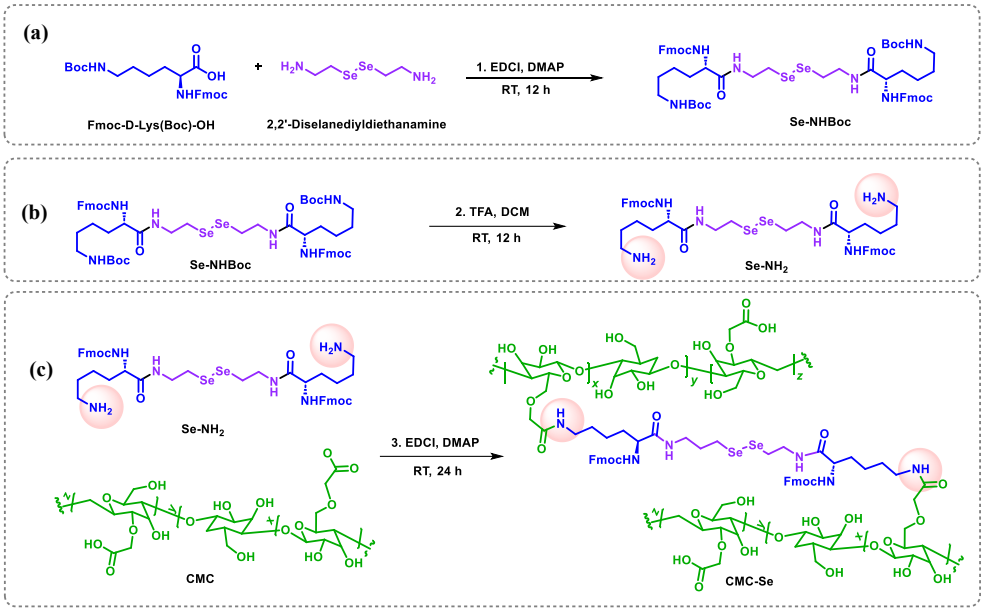

Scheme S1. Synthetic routes of Se-NHBoc (a), Se-NH_2 (b), and CMC-Se (c).

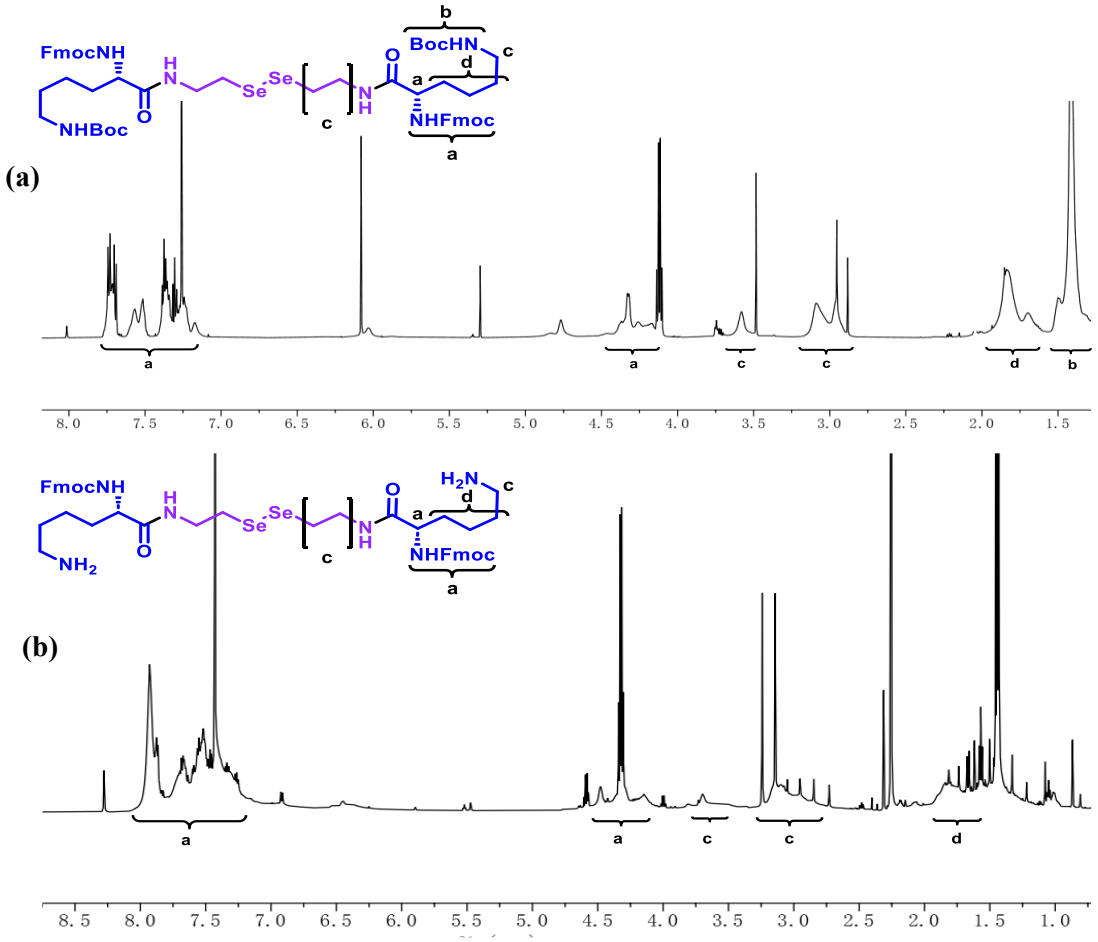

Figure S1. Chemical structure and ^{1}H spectrum of Se-NHBoc (a) and Se-NH_2 (b).

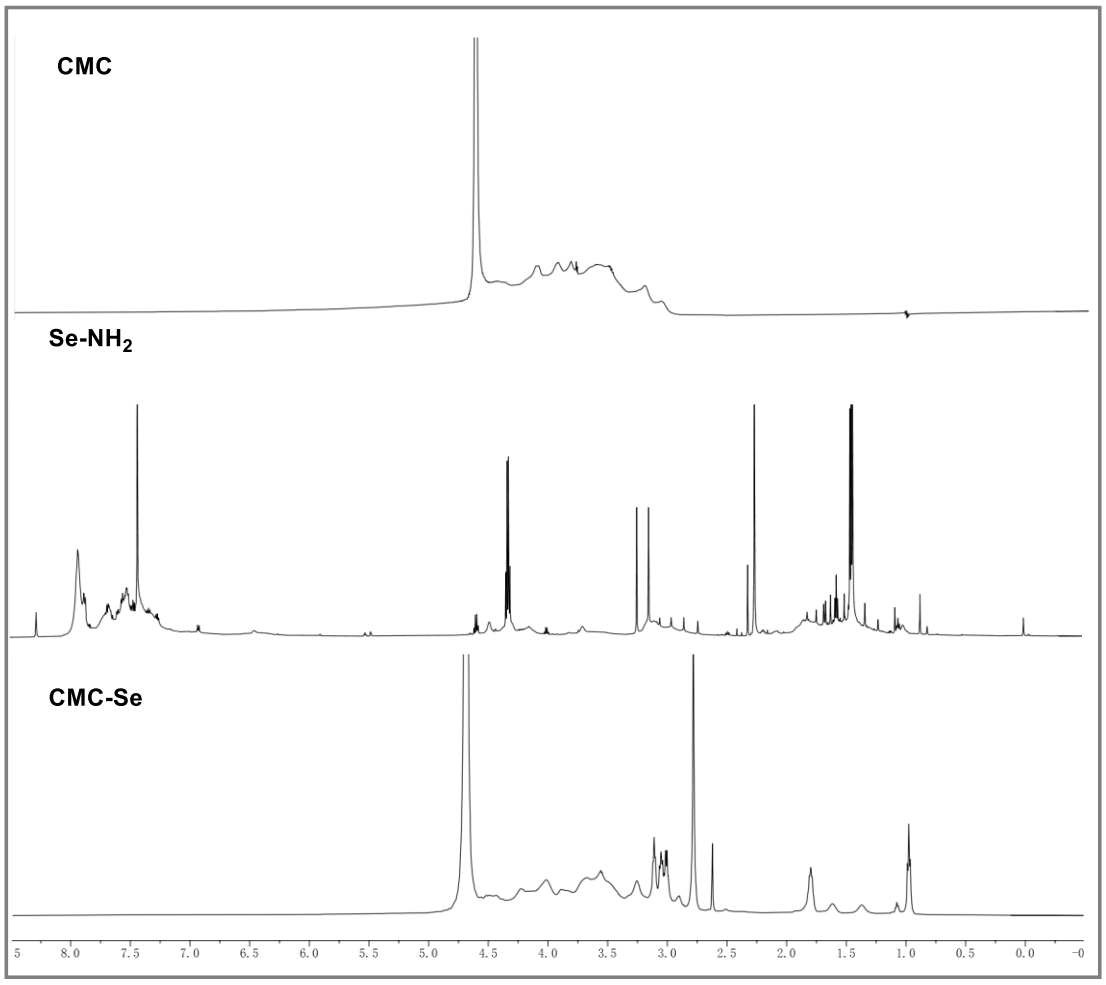

Figure S2. ^{1}H spectrum of CMC, Se-NH_2, and CMC-Se.

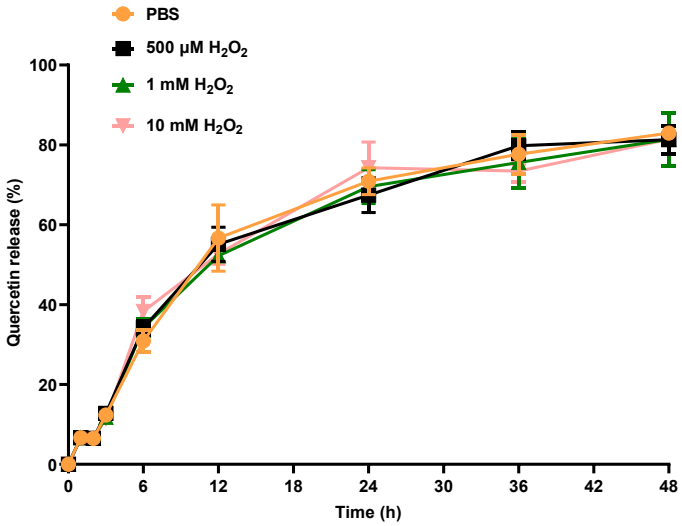

Figure S3. ROS responsive capability of CMC.

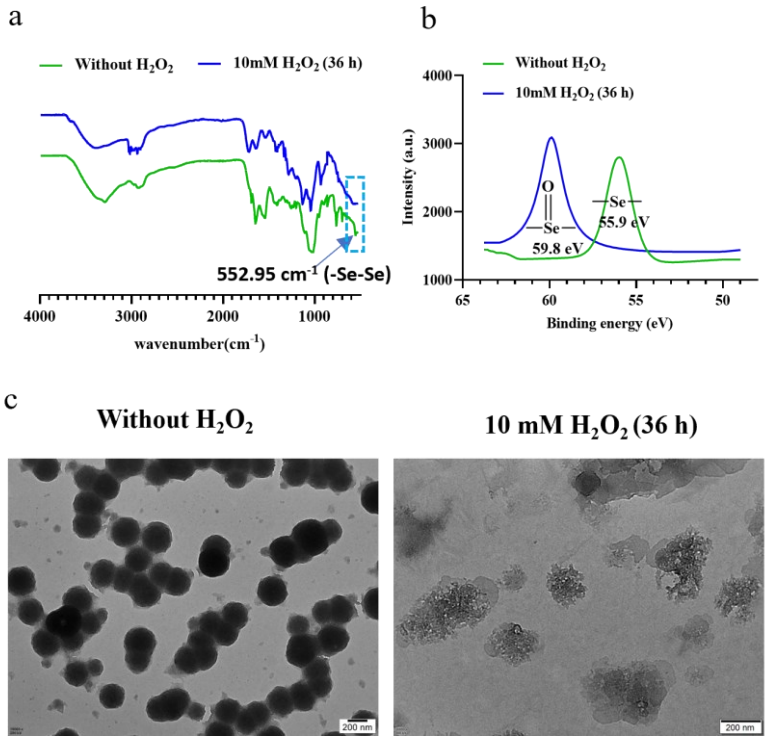

Figure S4. Characterization of CMC-Se with and without H_2O_2. FTIR analysis (a), XPS analysis (b), TEM images (c).

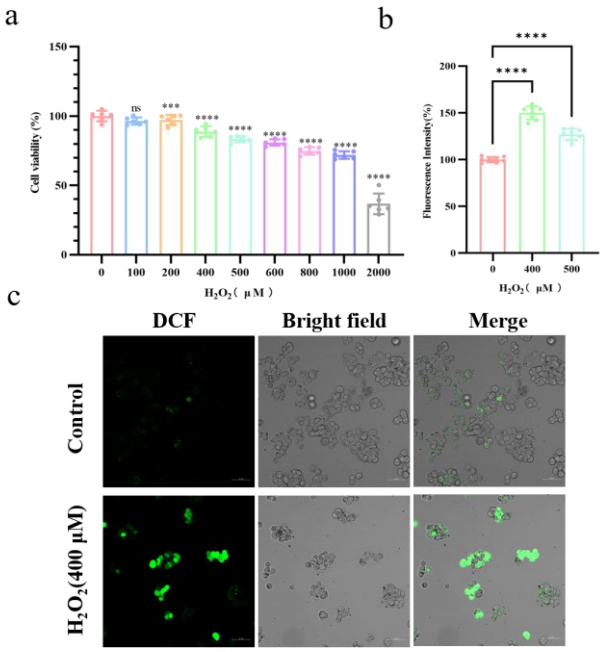

Figure S5. Cellular model of oxidative stressed HT-29 cells. Cell viability (a), ROS analysis (b), Fluorescence microscopy images (c). Data are displayed as mean ± standard deviation (SD) (n = 6). Statistical significance was assessed by one-way ANOVA and Tukey test. A probability value of $P < 0.05$ was considered statistically significant. $^{ns}P > 0.05$, $^{***}P < 0.001$, $^{****}P < 0.0001$.

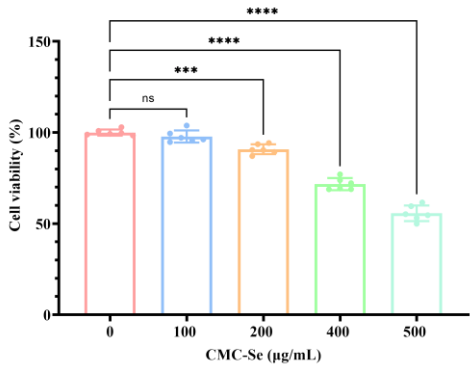

Figure S6. Cytotoxicity of CMC-Se in HT-29 cells. Data are displayed as mean ± standard deviation (SD) (n = 6). Statistical significance was assessed by one-way ANOVA and Tukey test. A probability value of $P < 0.05$ was considered statistically significant. $^{ns}P > 0.05$, $^{***}P < 0.001$, $^{****}P < 0.0001$.

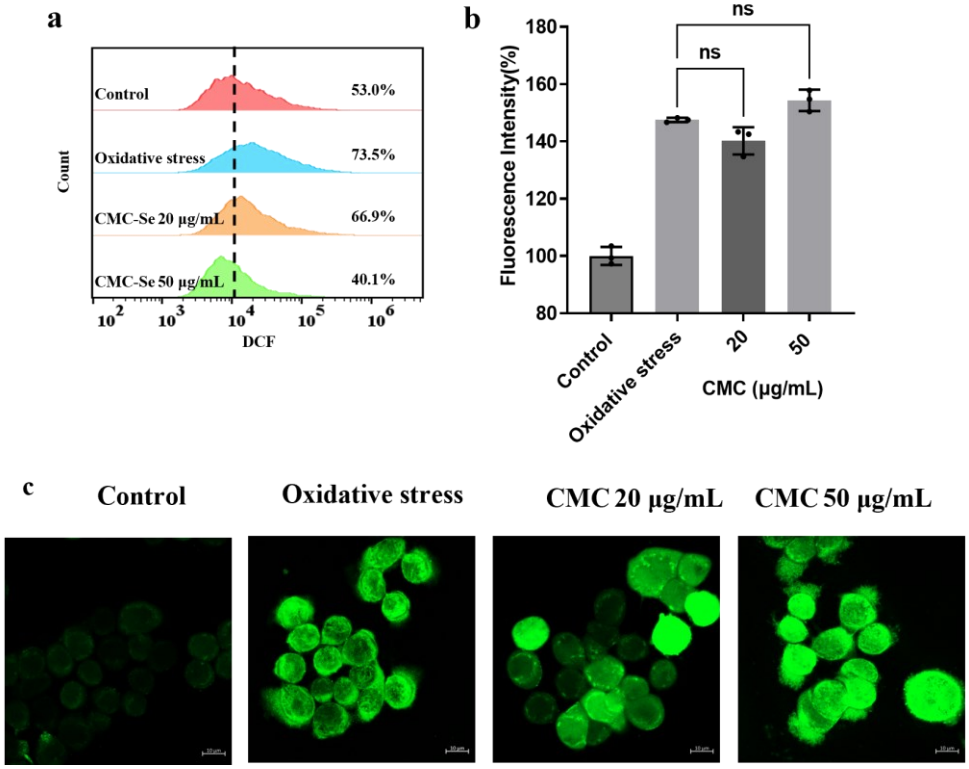

Figure S7. Flow cytometry analysis of intracellular ROS treated by CMC-Se in HT-29 cells (a), Microplate reader analysis of intracellular ROS treated by CMC in HT-29 cells (b), Confocal microscopy images of ROS treated by CMC in HT-29 cells (c).

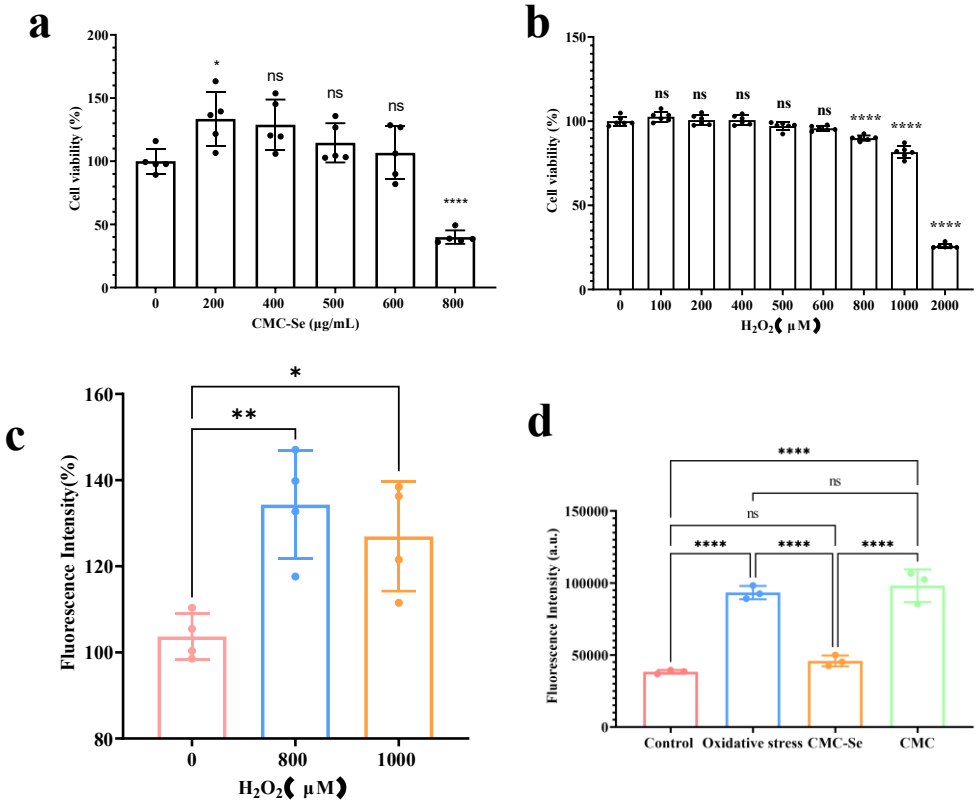

Figure S8. Cytotoxicity of CMC-Se in Caco-2 cells (a). Caco-2 Cellular model of oxidative stress. Cell viability (b), ROS analysis (c), Flow cytometry analysis of intracellular ROS (d).

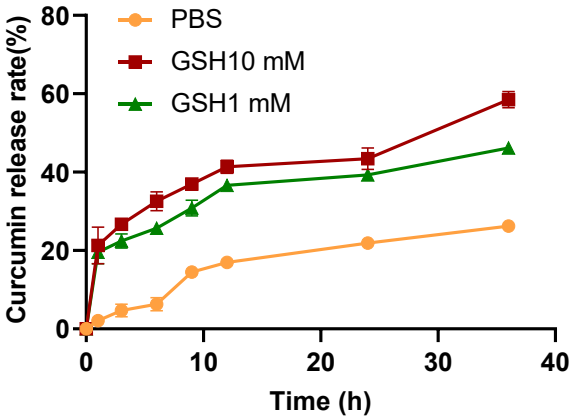

Figure S9. GSH responsive capability of CMC-Se.

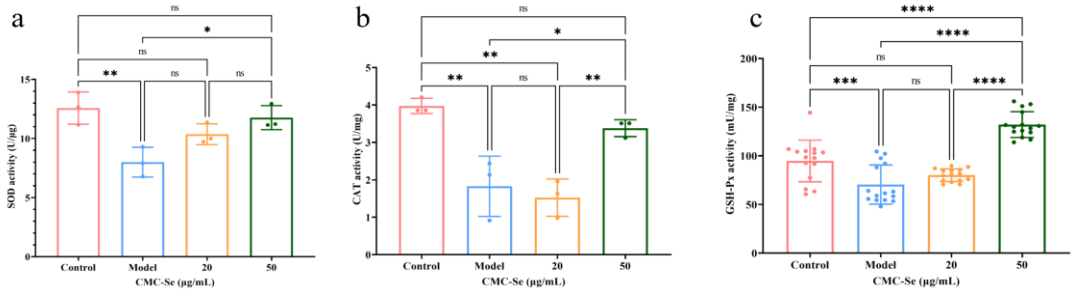

Figure S10. Effects of CMC-Se in oxidative stressed HT-29 cells. Enzyme activities of SOD (a), CAT (b), and GSH-Px (c). Data are displayed as mean ± standard deviation (SD) (n = 6). Statistical significance was assessed by one-way ANOVA and Tukey test. A probability value of $P < 0.05$ was considered statistically significant. $^{ns}P > 0.05$, $^{*}P < 0.05$, $^{**}P < 0.01$, $^{***}P < 0.001$, $^{****}P < 0.0001$.

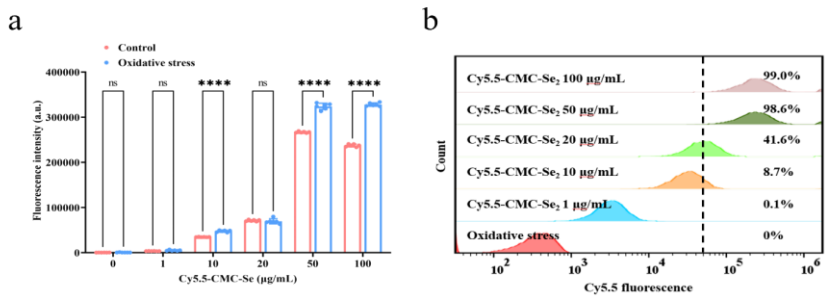

Figure S11. Flow cytometry analysis of CMC-Se cellular uptake. Average fluorescence quantification in normal or oxidative stressed HT-29 cells (a) and flow cytometry analysis in oxidative stressed HT-29 cells (b). Data are displayed as mean ± standard deviation (SD) (n = 6). Statistical significance was assessed by one-way ANOVA and Tukey test. A probability value of $P < 0.05$ was considered statistically significant. $^{ns}P > 0.05$, $^{*}P < 0.05$, $^{****}P < 0.0001$.

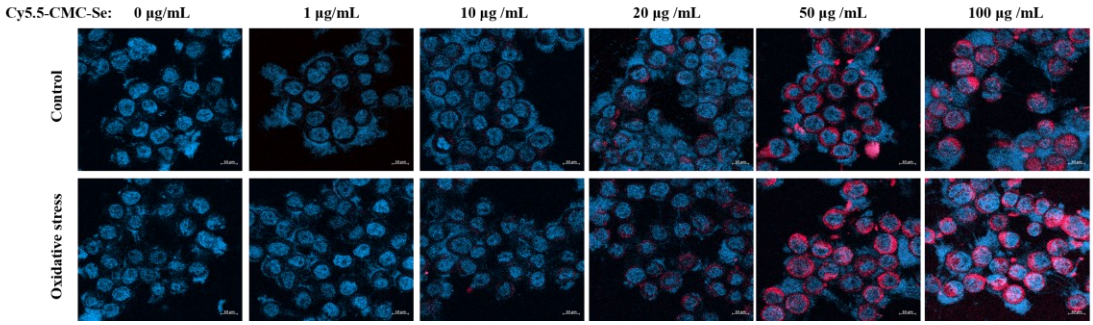

Figure S12. Confocal images of cellular uptake of CMC-se after treatment with different concentrations of CMC-Se in normal and oxidative stressed HT-29 cells. Scale bar: 10 μm

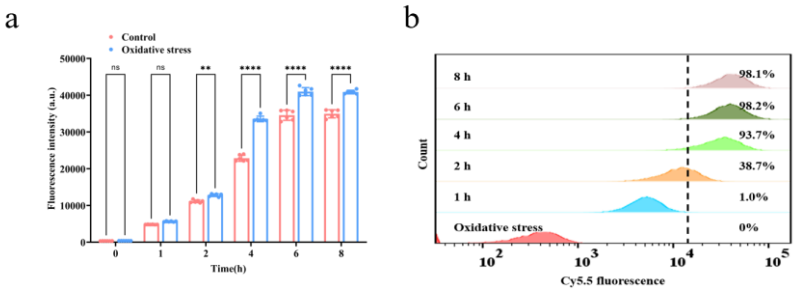

Figure S13. Flow cytometry analysis of CMC-Se cellular uptake after treatment with different time. Average fluorescence quantification in normal or oxidative stressed HT-29 cells (a) and flow cytometry analysis in oxidative stressed HT-29 cells (b). Data are displayed as mean ± standard deviation (SD) (n = 6). Statistical significance was assessed by one-way ANOVA and Tukey test. A probability value of $P < 0.05$ was considered statistically significant. $^{ns}P > 0.05$, $^{**}P < 0.01$, $^{****}P < 0.0001$.

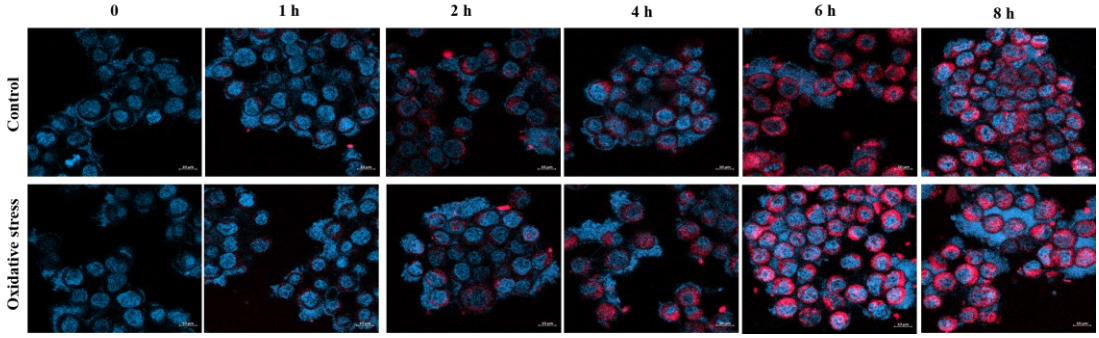

Figure S14. Confocal images of cellular uptake of CMC-Se after treatment with different times in normal and oxidative stressed HT-29 cells. Scale bar: 10 μm

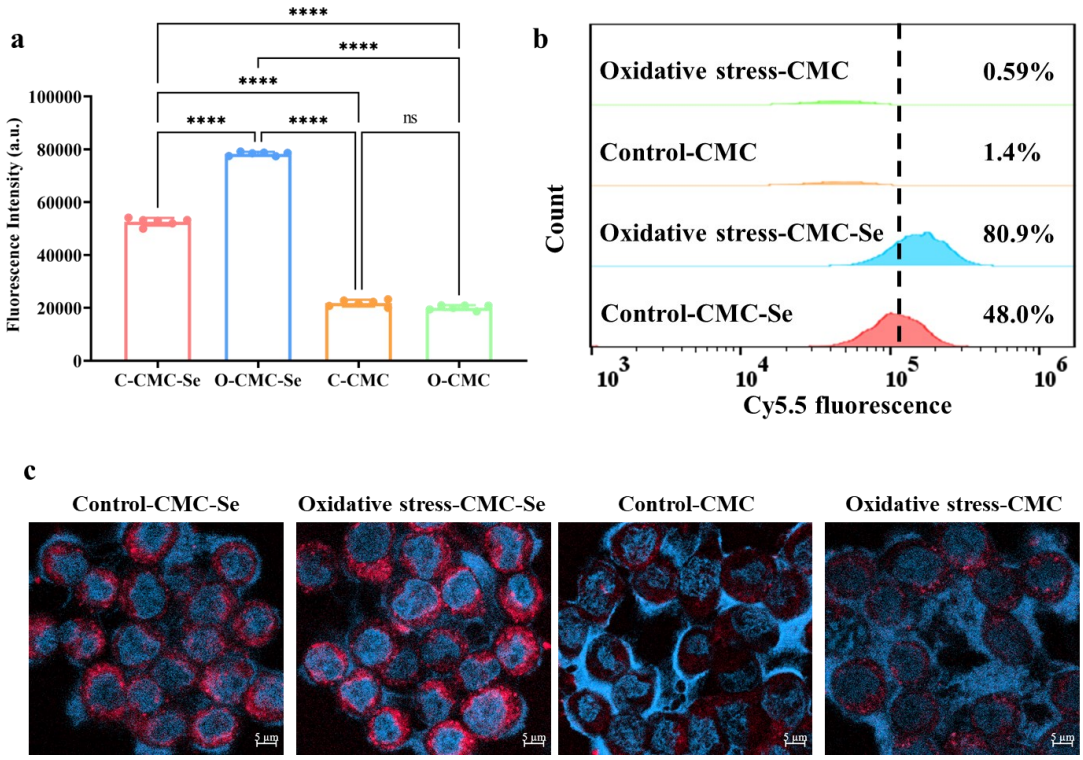

Fig. S 15. Comparative analysis of cellular uptake efficiency of CMC-Se and CMC in HT-29 cells. Flow cytometry analysis of cellular uptake of CMC-Se or CMC in normal or oxidative stressed HT-29 cells (a, b). Confocal images of cellular uptake of CMC-Se or CMC in normal or oxidative stressed HT-29 cells. Scale bar: 5 μm

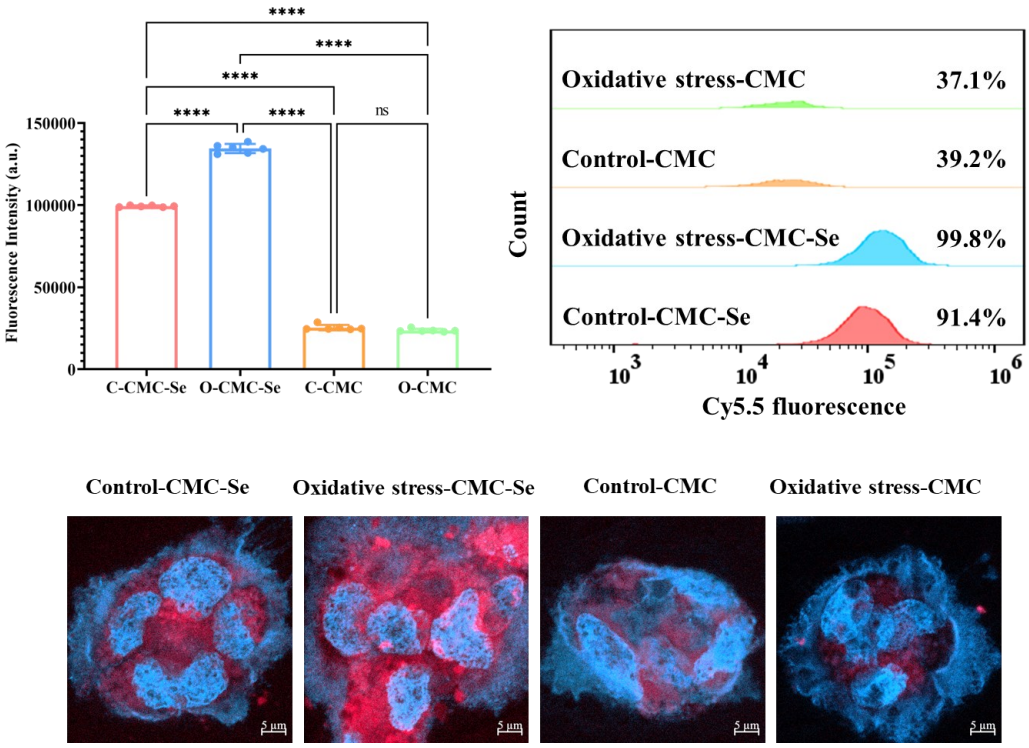

Fig. S16. Comparative analysis of cellular uptake efficiency of CMC-Se and CMC in Caco-2 cells. Flow cytometry analysis of cellular uptake of CMC-Se or CMC in normal or oxidative stressed Caco-2 cells (a, b). Confocal images of cellular uptake of CMC-Se or CMC in normal or oxidative stressed Caco-2 cells. Scale bar: 5 μm

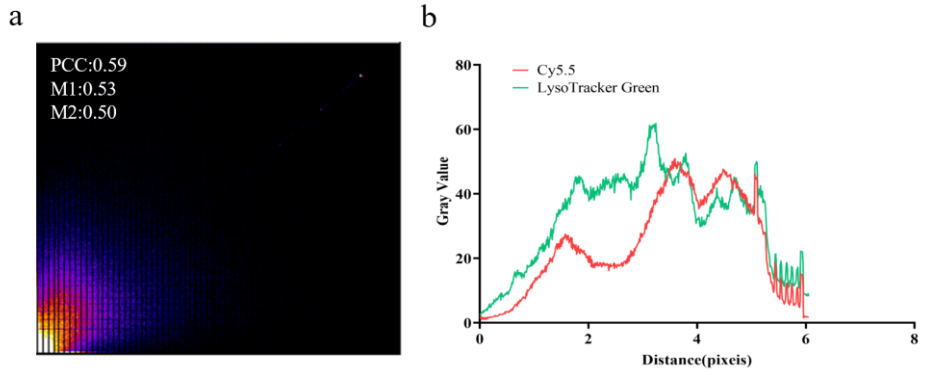

Figure S17. Colocalization analysis of lysosome. Analysis of PCC (Pearson correlation coefficient) and MCC (Mander's correlation coefficient) of Cy5.5-CMC-Se with lysosome (a). Spectrum analysis of Cy5.5-CMC-Se with lysosomes (b).

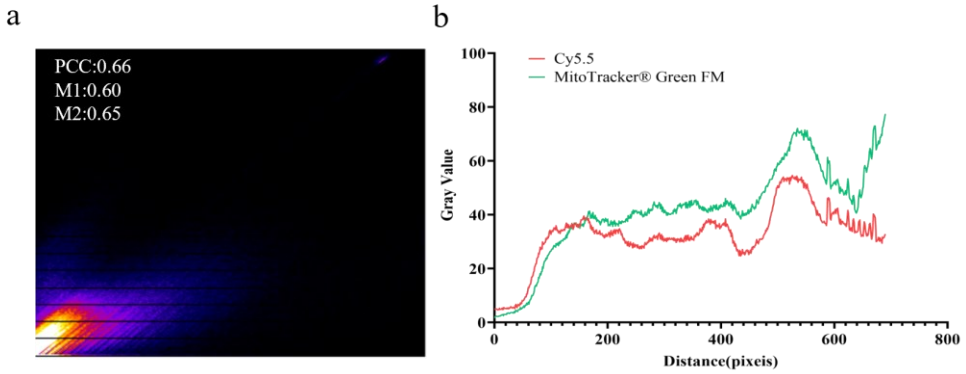

Figure S18. Colocalization analysis of mitochondria. Analysis of PCC (Pearson correlation coefficient) and MCC (Mander's correlation coefficient) of Cy5.5-CMC-Se with mitochondria (a). Spectrum analysis of Cy5.5-CMC-Se with mitochondria (b).

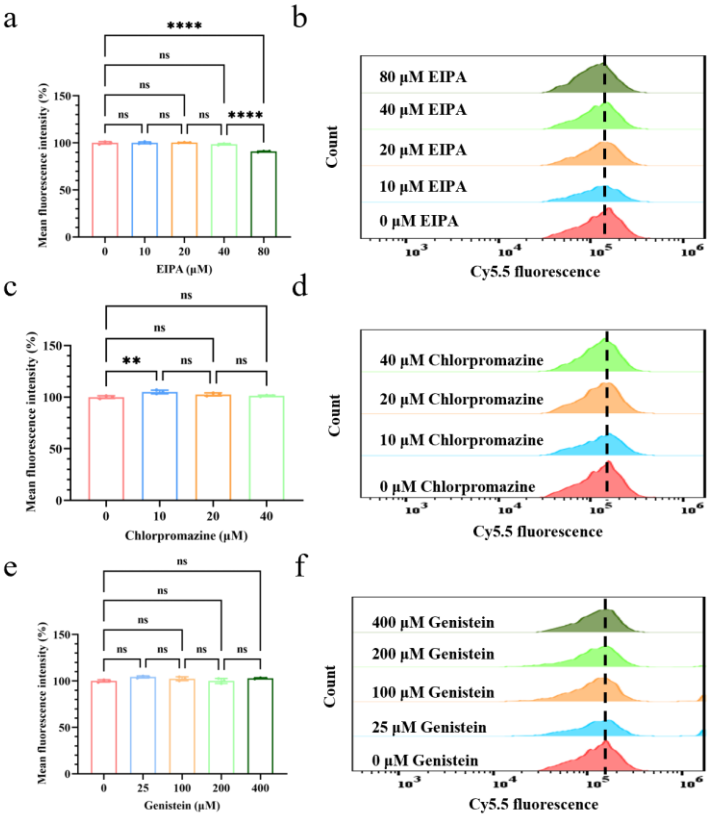

Figure S19. Effects of different inhibitors on cellular uptake in oxidative stressed HT-29 cells. Flow cytometry analysis of the effect of EIPA (a, b), Chlorpromazine (c, d), Genistein (e, f) on cellular uptake in oxidative stressed HT-29 cells after treatment with CMC-Se (50 μg/mL, 6 h). Data are displayed as mean ± standard deviation (SD) (n = 3). Statistical significance was assessed by one-way ANOVA and Tukey test. A probability value of $P < 0.05$ was considered statistically significant. *$^{ns}P > 0.05$, $^{**}P < 0.01$, $^{****}P < 0.0001$.*

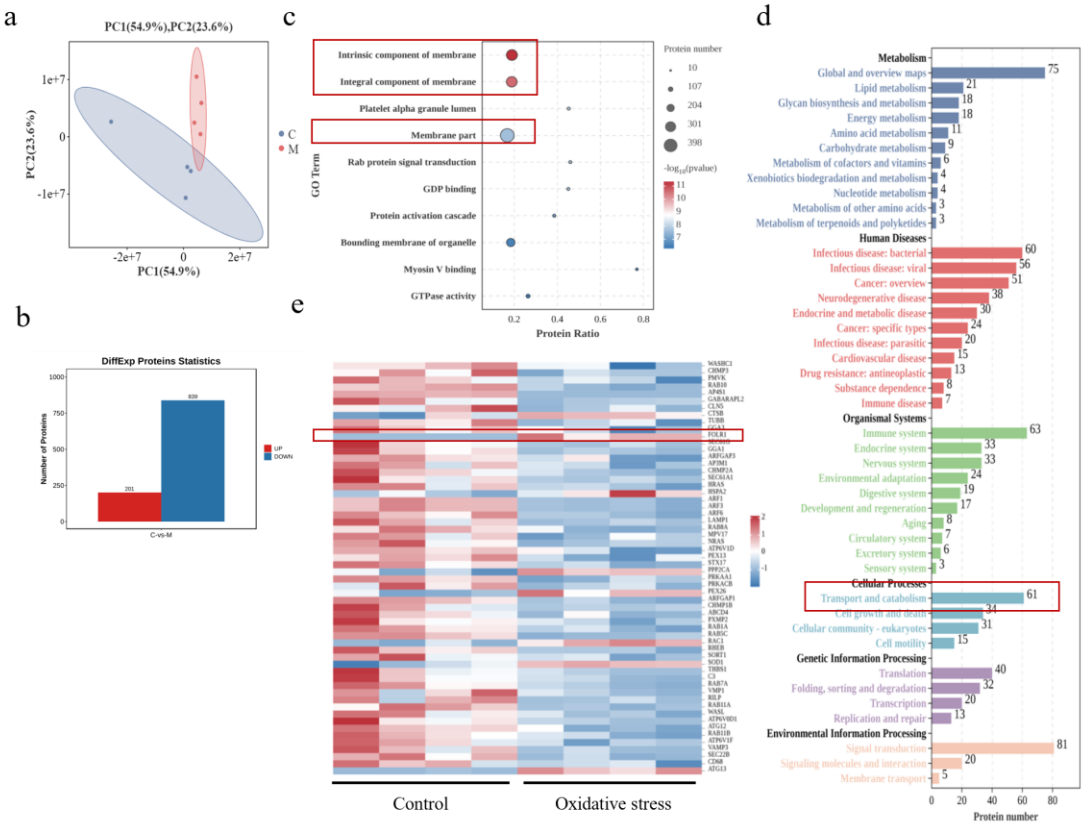

Figure S20. Proteomic analysis of cell membrane proteins of HT-29 Cells. PCA plot of protein expression between control and oxidative stress groups (a), the differential proteins between oxidative stress group cells and normal group cells (b), , GO analysis of DEPs between control and oxidative stress groups (c), KEGG enrichment analysis of DEPs associated with cell membrane or membrane function (d), Heatmap of DEPs related to transport and catabolism pathways (e).

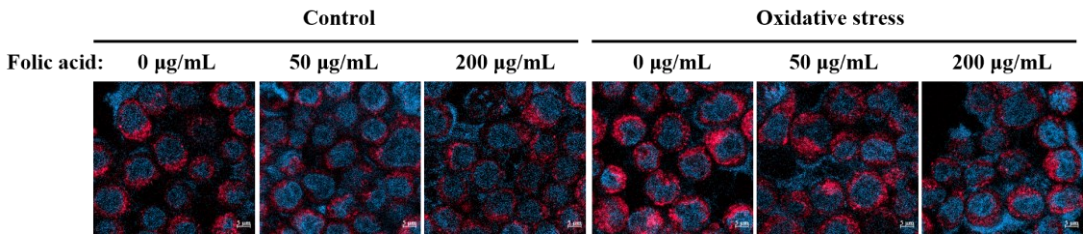

Figure S21. Confocal images of the effect of folate acid on the cellular uptake in normal or oxidative stressed HT-29 cells. Scale bar: 5 μm.

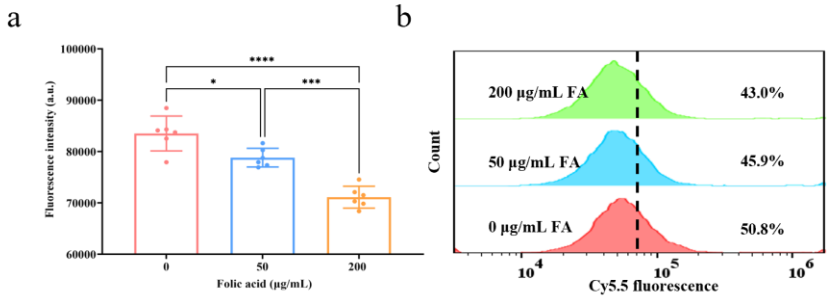

Figure S22. Flow cytometry analysis of the effect of folate acid on the cellular uptake in oxidative stressed HT-29 cells (a, b). Data are displayed as mean ± standard deviation (SD) (n = 6). Statistical significance was assessed by one-way ANOVA and Tukey test. A probability value of $P < 0.05$ was considered statistically significant. *$^{*}P < 0.05$, $^{***}P < 0.001$, $^{****}P < 0.0001$.*

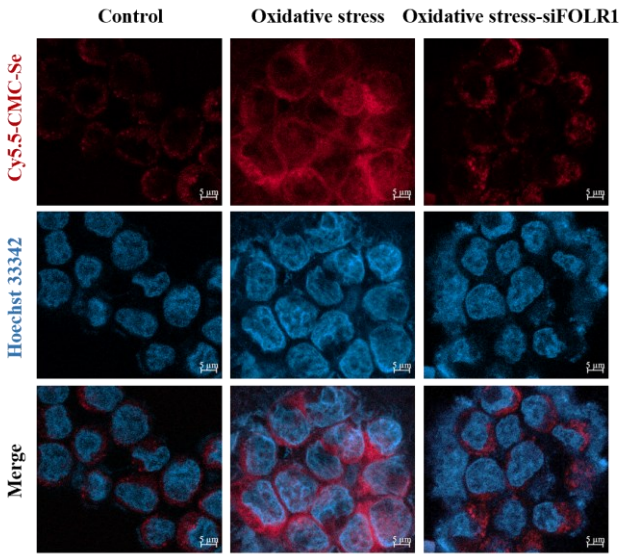

Figure S23. Confocal images of the effect of siFOLR1 on the cellular uptake. Scale bar: 5 μm.

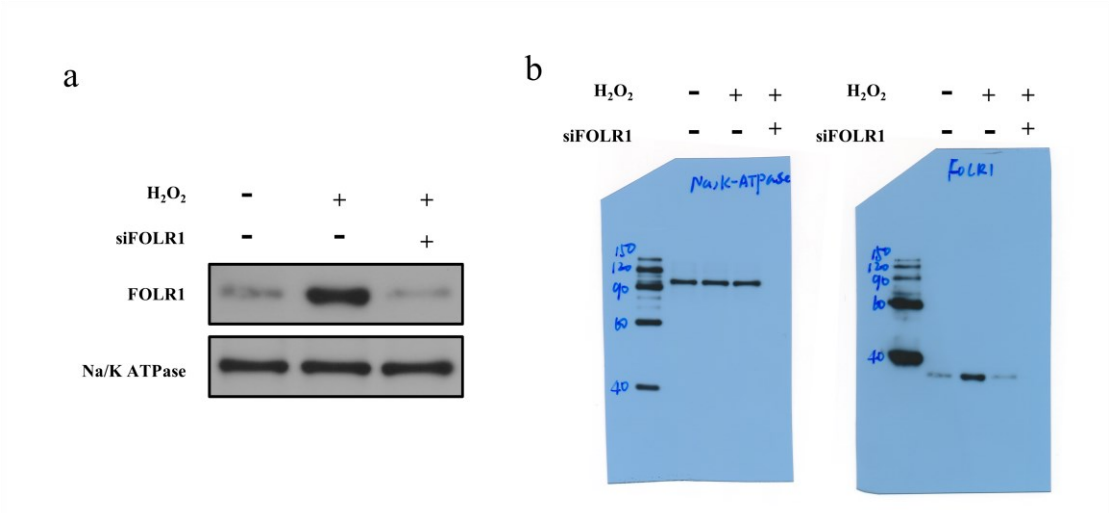

Figure S24. Western blot analysis of FOLR1 (a), raw image (b).

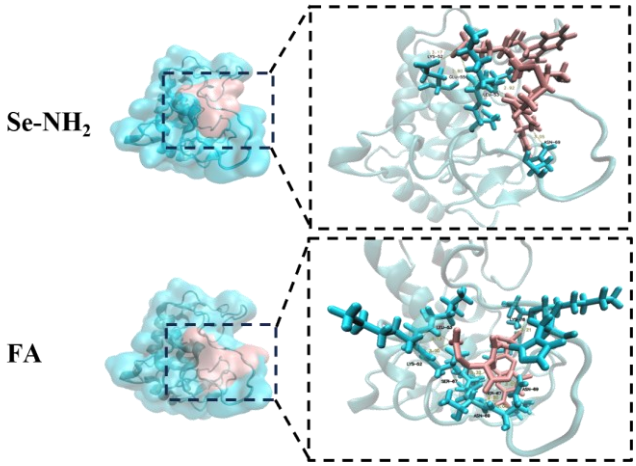

Figure S25. 3D docking model of folate or Se-NH_2 with folate receptor protein.